Kinetics and Mechanism of Coupling of Functionalized Chains at the Immiscible Polymer−Polymer Interface

Hideko T. Oyama and Takashi Inoue*

Department of Organic & Polymeric Materials, Tokyo Institute of Technology, Ookayama, Meguro-ku, Tokyo 152-8552, Japan

Received September 26, 2000; Revised Manuscript Received February 20, 2001

ABSTRACT: Theoretical and experimental studies in the literature on the coupling between functionalized polymer chains at immiscible polymer−polymer interfaces have always involved second-order kinetics. In addition, the time dependence of the degree of copolymer formation has been predicted to vary depending on the reaction stage. However, on the basis of careful reanalysis of the actual reaction orders in published work and our own experiments in the polyamide (aPA)/polysulfone (PSU) system, it is demonstrated that pseudo-first-order kinetics in the parameter ($\Sigma^* - \Sigma$) are universally obtained over the whole time scale. The quantities Σ and Σ^* are respectively the areal density of copolymers formed at time t and at infinite time at the interface. It indicates the time dependence of $\Sigma \sim -\exp(-t)$ at all stages. On the basis of these results, a new reaction model is proposed, in which coupling is viewed as involving the formation of a two-dimensional monolayer on the interface surface by copolymers formed in situ. The coupling process giving rise to the pseudo-first-order kinetics is considered to be reaction-controlled.

Introduction

Copolymers generated in situ in "reactive processing" at the interface between immiscible polymers play an important role in stabilizing polymer blends by reducing the interfacial tension, inhibiting particle coalescence, and improving interfacial adhesion.[1−3] There have been many papers published to prove the effectiveness of these copolymers in fortifying morphology and improving the properties of the resultant polymer blends. This activity was initiated by the discovery in 1974 of the stability of blends of polyamide/polypropylene (PP) functionalized with maleic anhydride blends.[4] However, despite the passage of a quarter of a century since this finding, basic knowledge on the kinetics of the coupling reaction at the interface is still lacking. In the past several years, fundamental approaches in theory and experiments have just started to be reported.

Fredrickson[5,6] and O'Shaughnessy and Sawhney[7,8] independently reported theoretical results on the kinetics of the coupling reaction held at the immiscible polymer−polymer interface. For simplicity, it was assumed in both treatments that the chains were symmetric in size (the degree of polymerization, $N_A = N_B = N$), a flat interface was formed between them under quiescent conditions, and reactive groups were located at one chain end of the two polymers.

Their studies predicted that in the initial reaction stage the number of copolymer chains per area, Σ, would increase in time t, following second-order kinetics:

$$\frac{d\Sigma}{dt} = K(t) n_A n_B \qquad (1)$$

where $K(t)$ was the rate constant and n_A and n_B were the number density of reactive chains carrying the reactants A and B, respectively. Fredrickson and Milner proposed three time regimes on the basis of the assumption that diffusion of the reactive chains would control the overall reaction kinetics:[6] an initial regime where the density of reactive chains in the interfacial region could be considered to be the same as the value in the bulk, an intermediate regime where there was a depletion hole of reactants in the interfacial region so that the reaction was controlled by center-of-mass diffusion of reactive homopolymers to the interface, and a late regime where interfacial saturation by resultant copolymers suppressed the reaction. The predicted time dependence was a linear growth of Σ in t in the initial time regime, a $t^{1/2}$ growth in the intermediate regime, and a $(\ln t)^{1/2}$ growth in the late regime. In the late regime, the copolymers would be severely stretched compared to the unperturbed coil size and a significant chemical potential barrier ($\gg k_B T$) would develop for reactive chains to further react.

Furthermore, O'Shaughnessy and Sawhney categorized the reaction depending on the reactivity of the functional groups and the stage of the reaction.[8] For example, it was predicted that in the reaction with weakly reactive pairs at the beginning, the reaction rate constant, $K(t)$, would obey mean field theory resulting in $K(t) = Qa^3h$ ($\sim h$), where Q, a, and h were the local functional group reactivity, the reactive group size, and the interfacial thickness, respectively. On the contrary, in the reaction with strongly reactive pairs at the beginning, $K(t)$ would be controlled by the diffusion process of the reactants. At $N < N_e$ (the degree of polymerization to start forming chain entanglements), $K(t) = (a^4/t_a)[1/\ln(R/h)]$ ($\sim 1/(\ln N)$), and at $N > N_e$, $K(t) = (a^4/t_a)(1/[(N/N_e)(\ln(N/N_e)])$ ($\sim 1/(N \ln N)$), where R and t_a were the coil size and the relaxation time of a single chain unit, respectively. Finally, at the end of the reaction the effects of interfacial saturation would become significant, so that if Σ exceeded $N^{-1/2}a^{-2}$ ($\equiv \Sigma_{crit}$), $K(t)$ would be suppressed as $\sim\exp(-\text{const}(\Sigma/\Sigma_{crit})^2)$.

In further work, O'Shaughnessy and Vavylonis introduced four types of reaction kinetics and three distinct kinetic sequences, which gave rise to different types of reaction kinetics as a function of time.[9,10] For example, in short-time ranges for common reactions

* To whom inquires should be addressed. Tel/FAX +81-238-26-3060; e-mail tinoue@dip.yz.yamagata-u.ac.jp.

10.1021/ma001672c CCC: $20.00
Published on Web 04/13/2001

Table 1. Sample Characteristics

sample	M_n (g/mol)	M_w (g/mol)	T_g (°C)	functionality	
				μmol/g	no./chain
nf-PSU	6050	20 120	170	0	0
PSU-ω-PAH	7000	19 700	164	143	1.00
PSU-ω-triazine	6200	19 740	172	102	0.63
aPA	8400	32 800	97	119	1

with small reactivity, second-order reaction-controlled kinetics with $\Sigma \sim t$ following mean field theory would be observed until interfacial saturation was reached. On the other hand, in reactions with high reactivity, a transition from second-order reaction-controlled kinetics to first-order diffusion-controlled kinetics would occur at short times. In this time regime, it was predicted that $\Sigma \sim t/(\ln t)$ for unentangled chains and $\Sigma \sim t/(\ln t)$ and $t^{1/2}$ regimes for entangled chains. In long-time kinetics, first-order diffusion-controlled kinetics would be observed, in which $\Sigma \sim t^{1/4}$ for unentangled chains and $\Sigma \sim t^{1/4}$ and $t^{1/8}$ regimes for entangled chains. Finally, in cases involving interfacial saturation, first-order diffusion-controlled kinetics with $\Sigma \sim t^{1/2}$ were predicted.

Although quantitative experiments to investigate the coupling reaction at the immiscible polymer interface are still rare, some results have been reported under quiescent conditions.[11−14] Most experimental results were analyzed using second-order kinetics without a precise check of the actual reaction order. The initial slope in a plot of Σ vs time was often used for determination of a rate constant. To shed light on this problem, the experimental results on the coupling reaction at the polymer interface will be further discussed in later sections.

In this paper the kinetic order observed in experiments is given the label "pseudo-". This is to account for cases such as in eq 1 where second-order kinetics become "pseudo-first-order", when one of the concentration terms is constant. In other papers the kinetic order is simply given by the sum of exponents in the concentration terms of the kinetic equation.

In this paper we will first present experimental results on the interfacial reaction in various systems. It will be demonstrated that the pseudo-first-order kinetics are widely observed as the apparent kinetic order. Then, it will be shown that a general treatment in surface science used for reactions at the gas/solid interface can be effectively applied to the reaction at the polymer−polymer interface. The present approach is unique. All other theoretical studies have their basis on other foundations, such as diffusion of reactive polymer chains and the mean field approximation considering the chemical potential of reactive chains.

Experimental Section

The specimens and characteristics of the polymers used in this study are listed in Table 1 and depicted in Figure 1. In addition to nonfunctionalized PSU (nf-PSU), two different types of PSUs functionalized with phthalic anhydride (PAH) and with triazine at the chain ends (ω) were prepared by following synthetic procedures given in the literature.[15,16] Amorphous polyamide (aPA) containing one terminal primary amine group per chain was obtained from EMS Japan.

Bilayer films consisting of an aPA layer of ca. 0.5 mm thickness and a PSU layer with 200−500 nm thickness were prepared using a method described previously.[17] After the bilayer film was annealed at 200 °C for a given time, the PSU layer was thoroughly removed by chlorobenzene, and the exposed interface on the aPA side was analyzed by X-ray photoelectron spectroscopy (XPS) for determination of the areal

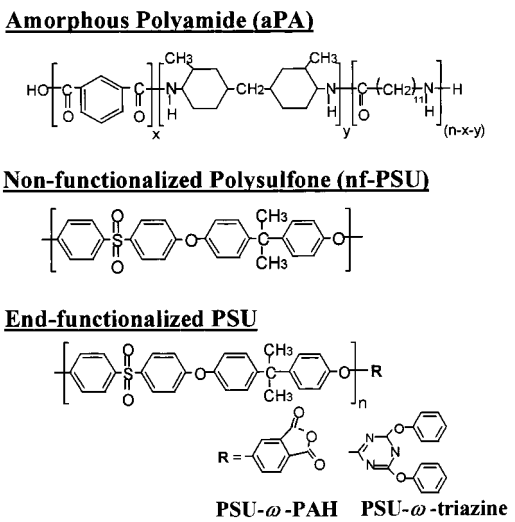

Figure 1. Chemical structures of PSU and aPA samples.

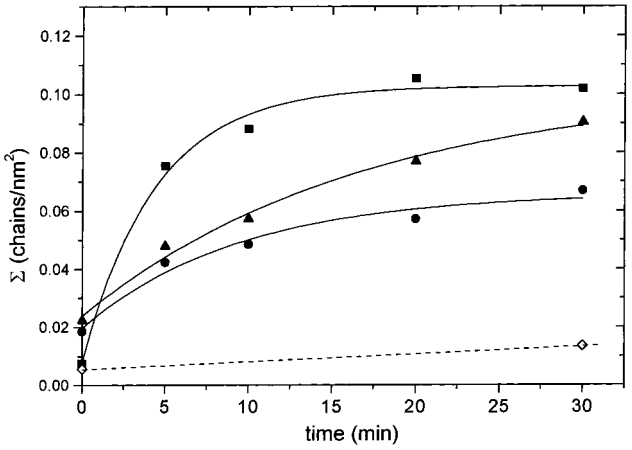

Figure 2. Areal density of copolymers formed in situ at the interface, Σ (chains/nm^2), when the bilayer specimen was heated at 200 °C for a given time. The solid lines indicate the first-order fit. aPA/PSU-ω-PAH (■), aPA/PSU-ω-triazine (●) with the PSU functionality of 55 μmol/g, aPA/PSU-ω-triazine (▲) with the PSU functionality of 102 μmol/g, and aPA/nf-PSU (◇).

density of copolymers formed in situ at the interface, Σ. The characteristic photopeaks of the N 1s from aPA and the S $2p_{3/2}$ from PSU were used as probes. From the atomic ratio of S to C and that of N to C of the exposed interface, the amount of the PSU comonomer covering the aPA surface could be estimated, and from this the Σ value could be easily calculated.[18] The unit employed for the measurements was a Perkin-Elmer PHI 5500.

The value of saturation areal density of copolymer, Σ^*, was estimated by the best fit of the experimental data to the first-order equation in $(\Sigma^* - \Sigma)$ using a fitting program. It was found that this method gave us a reasonable Σ^* value even for cases where the experimental range of Σ did not reach saturation.

Results

PSU/aPA. Figure 2 shows the change in the areal density of copolymers, Σ (chains/nm^2), generated at the interface, when the bilayer films of aPA/reactive PSU were annealed at 200 °C for a given time. The values shown in the figure were obtained by averaging the Σ values calculated from the content of N, a characteristic element of aPA, and the content of S, a characteristic element of PSU, observed at the exposed interface by X-ray photoelectron spectroscopy (XPS). (In the case of the PSU-ω-triazine system with contribution of the

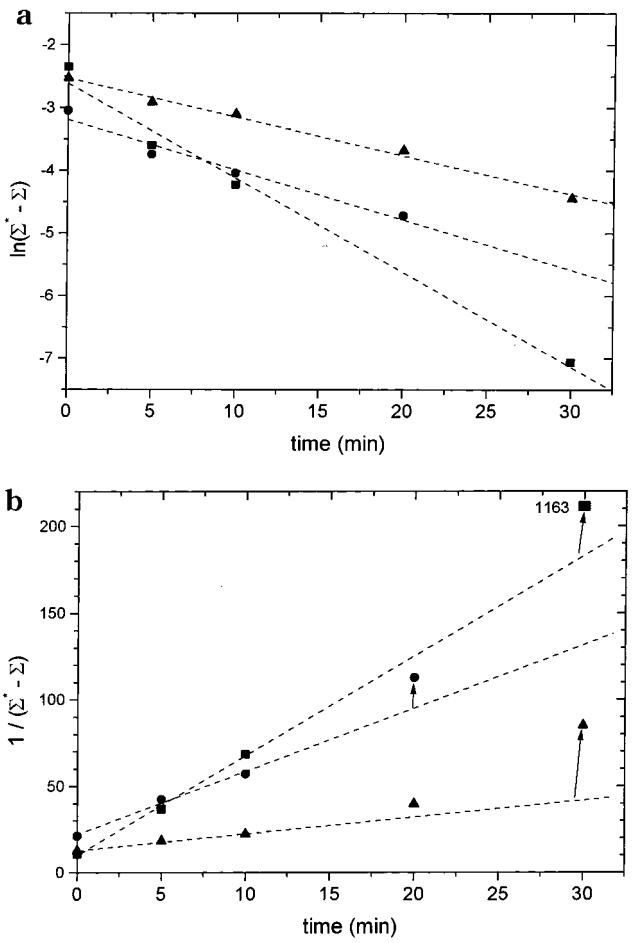

Figure 3. (a) First-order plot and (b) second-order plot of the data shown in Figure 2. (■), (●), and (▲) are the same as Figure 2.

functional group to the N content, the Σ was estimated only from the content of S.) The structures of PSU-ω-PAH and PSU-ω-triazine with the PSU functionality of 55 μmol/g are almost identical except for the reactive groups attached to them. Data for those polymers are labeled ■ and ●, respectively. It is expected that diffusion of the reactive chains to the interface will be similar in both cases. A comparison between two different PSU-ω-triazine samples indicates that Σ is enhanced by an increase in the concentration of the reactive PSU chains.

The positive Σ values observed at $t = 0$ are probably caused by some intermolecular interactions between the two component polymers, e.g., hydrogen bonding between the amide linkage of aPA and S═O and −O− groups of PSU, since the positive Σ values were also observed in the nonreactive aPA/nf-PSU.

The reaction kinetics were examined by carrying out first-order (Figure 3a) and second-order (Figure 3b) analyses, based on the assumption that the reaction rate would vary with (Σ* − Σ). In this case, it was assumed that the coupling reaction would be terminated at Σ = Σ*. The results given in Figure 3 clearly indicate that the reaction followed first-order kinetics in (Σ* − Σ) over the whole time scale.

The coupling kinetics at the immiscible polymer interface has usually been treated as second-order largely because the reaction is bimolecular, and the order of the reaction kinetics has seldom been checked in the literature. Therefore, the analysis of the kinetics was also extended to data already reported by other groups.

First, a search was undertaken for experimental data on simple coupling reactions between two end-functionalized chains (one reactant/chain). Although data were found for the reaction between amino-terminal deuterated polystyrene (dPS-NH_2) and anhydride-terminated poly(methyl methacrylate) (PMMA-anh) monitored by forward recoil spectroscopy (FRES),[14] the data were too scattered to be used for the determination of the order of the reaction kinetics. That is the reason why only data involving complicated interfacial reactions are cited below.

SMA/ATBA. Scott and Macosko reported the interfacial reaction monitored by Fourier transform infrared spectroscopy (FTIR).[11] The formation of imide was observed using bilayer specimens composed of styrene−maleic anhydride copolymer (SMA) with 17 wt % of maleic anhydride (MA) and butadiene−acrylonitrile copolymer (ATBA) containing 16 wt % of acrylonitrile and the NH_2 group located at both chain ends, as shown in Figure 4a.

For the analysis it was assumed that Σ ∼ area (imide) measured by IR, and the latter quantity was used for the calculations. This substitution does not affect the determination of the kinetic order or the activation energy. It was demonstrated by the first-order plot (Figure 4b) and the second-order plot (Figure 4c) that the interfacial reaction again followed first-order kinetics in (Σ* − Σ) over the whole time scale. It is important to emphasize that simple first-order kinetics were observed despite the complicated architecture of the resultant copolymers, in which both ends of the ATBA chain reacted with MA groups along the SMA chain.

The slope of the lines shown in Figure 4b implies that the reaction rate constant at 160 °C was almost 5 times larger than that at 140 °C. The activation energy was estimated to be 120 kJ/mol using the reaction rate constants determined from the slopes in Figure 4b. The reactant concentration was quite high in this experiment; [MA] of SMA = 1.7×10^3 μmol/g and [NH_2] of ATBA = 5×10^2 μmol/g.

SMA/Nylon 11. Scott and Macosko further examined imide formation at the interface between the same SMA and nylon 11 (M_n = 1535 and 5141), as given in Figure 5a.[11] First-order (Figure 5b) and second-order (Figure 5c) analyses for this reaction were also carried out, and it was found that the interfacial reaction again followed first-order kinetics in (Σ* − Σ) in the whole time scale. The concentrations of the reactants were quite high in this system; [MAH] of SMA was the same as that in the previous SMA/ATBA system, and [NH_2] of nylon 11 = 1.3×10^3 and 3.9×10^2 μmol/g for M_n = 1535 and 5141 g/mol, respectively. The slopes of the two lines in Figure 5b were almost the same, indicating that the rate constants were similar for the two reactions. Even though the initial slopes of the two data sets in Figure 5a were quite different, the rate constant in (Σ* − Σ) was almost the same.

PS−COOH/Precured Epoxy Containing Extra Epoxide. Kramer analyzed the interfacial reaction between polystyrene terminated with carboxylic acid groups (the COOH is denoted as reactive group A here) and precured epoxy containing extra epoxide (denoted as reactive group B), as shown in Figure 6.[12,13] It was concluded in his work that the reaction-controlled model fit the data better. According to Kramer's model, the

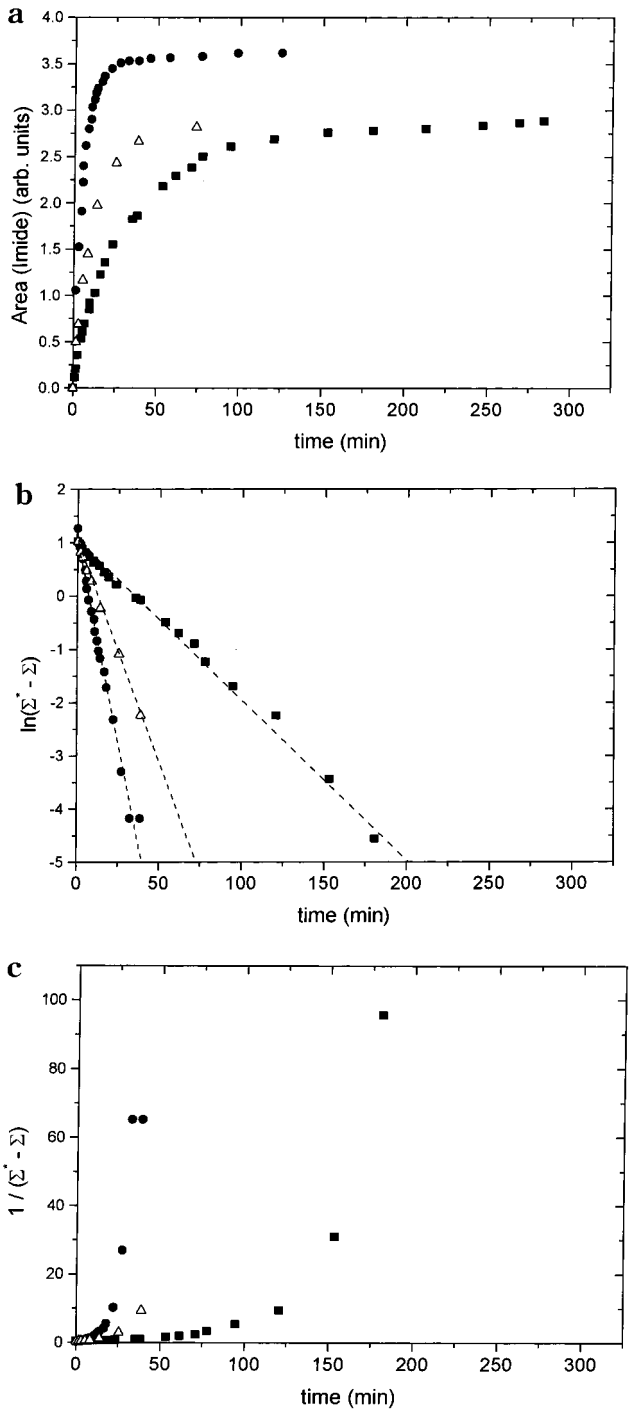

Figure 4. Reaction at the SMA/ATBA interface reported in ref 11. (a) Amount of imide formation vs time; (b) the first-order plot; (c) the second-order plot [●, reaction at 160 °C; △, at 150 °C; and ■, at 140 °C].

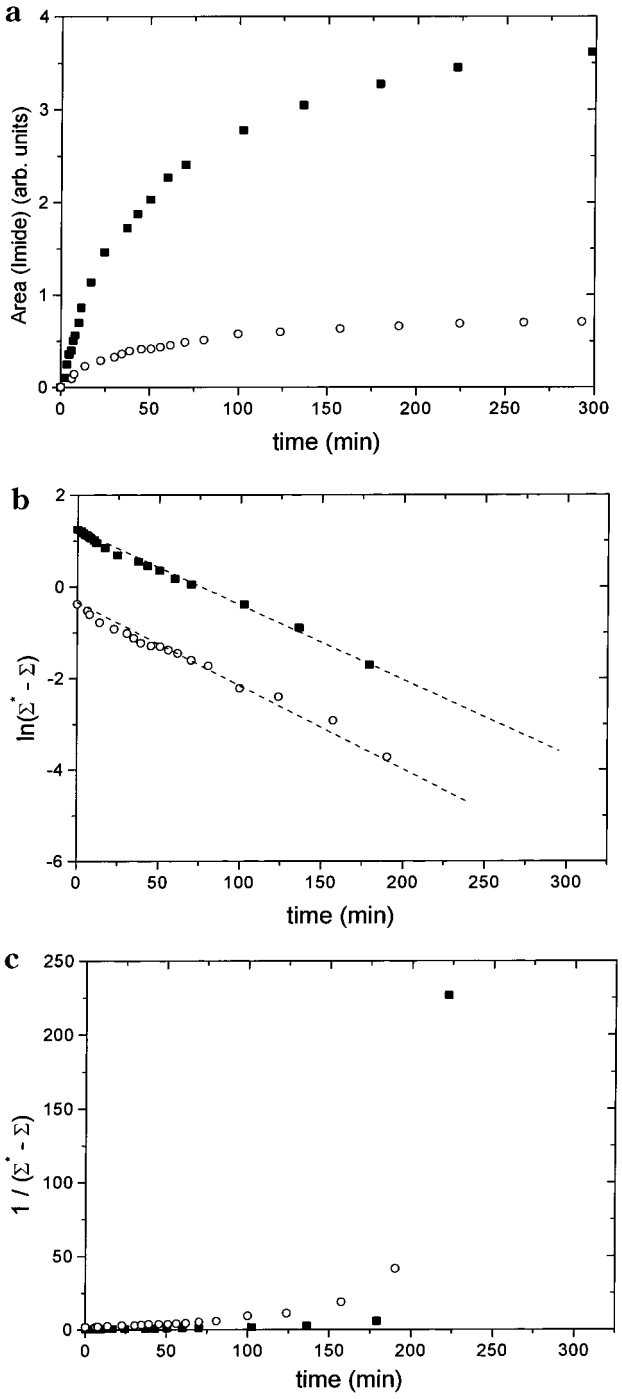

Figure 5. Reaction at the SMA/nylon11 interface reported in ref 11. (a) Amount of imide formation vs time; (b) the first-order plot; (c) the second-order plot [■, reaction at 180 °C with low MW of nylon 11; ○, reaction at 190 °C with high MW of nylon 11].

reactant concentration of B at the interface, $[B_{interface}]$, was assumed to be constant and that of A, $[A_{interface}]$, to be a variable. In addition, the effect of copolymer brush formation on the chemical potential to form the $A_{interface}$ was taken into consideration, based on a self-consistent-field theory developed by Shull.[19]

The figure clearly demonstrates that Kramer's model shown as the solid line, in which reaction rate decreases as a function of $1/\exp(\Sigma^2)$, tends to overestimate the Σ value in short time scales and to underestimate it in long time scales. In contrast, the data agree quite well in the whole time scale with the first-order fit, shown as the dashed line, obtained by assuming that the reaction rate decreases linearly with decrease of $(\Sigma^* - \Sigma)$.

In this section it has been demonstrated that the apparent coupling kinetics at the immiscible polymer–polymer interface do not necessarily follow a second-order dependence. For a number of cases it was shown that pseudo-first-order kinetics in $(\Sigma^* - \Sigma)$ was often observed, including a system consisting of multifunctional polymer chains. In the next section, the coupling kinetics and mechanism will be discussed by proposing new reaction models while clarifying the meaning of $(\Sigma^*$

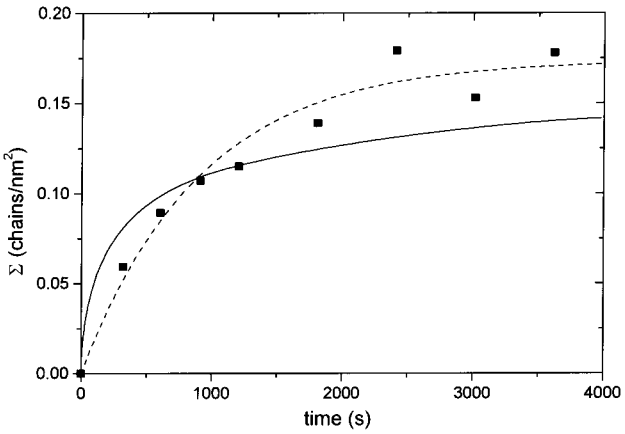

Figure 6. Grafting density of PS−COOH onto epoxy-rich cross-linked epoxy. [Kramer's model[13] (solid line) and the first-order fit in ($\Sigma^* - \Sigma$) (dashed line)].

$- \Sigma$) used for the analysis to determine the order of the reaction kinetics.

Discussion

Processes in the Coupling Reaction. For the case where a single copolymer is formed between one A group and one B group, the overall coupling reaction is assumed to involve the following processes. In the equations below, $[A_{interface}]^0$ denotes the initial concentration of reactive sites A located at the interface and $[B_{interface}]^0$ represents the initial concentration of reactive sites B located at the interface.

Initial conditions: the reactive groups of $[A_{interface}]^0$ and $[B_{interface}]^0$ are present at the interface.

$$\text{interface} + A_{bulk} \rightleftarrows A_{interface} \quad (2)$$

$$\text{interface} + B_{bulk} \rightleftarrows B_{interface} \quad (3)$$

$$A_{interface} + B_{interface} \rightarrow A{-}B_{interface} \quad (4)$$

It is assumed that $[A_{interface}]^0$ and $[B_{interface}]^0$ are proportional to the reactant concentrations in the bulk, $[A_{bulk}]$ and $[B_{bulk}]$, respectively. The processes shown by eqs 2 and 3 are controlled by diffusion, whereas that shown by eq 4 is controlled by reaction.

Assumptions for Modeling. Four assumptions were made in order to explain the mechanism of the coupling reaction: (1) *A flat interface* is formed between the polymers. (2) The copolymers formed by the reaction *stay stably at the interface.* (3) The coupling reaction proceeds *two-dimensionally* on the interface plane. (4) *A monolayer-like* quantity develops at the interface.

The first assumption means that the interfacial area is considered to be constant during the coupling reaction. It is recognized that an undulated interface is sometimes formed at high copolymer density in order to diminish the entropic penalty associated with a densely packed copolymer brush formed at the interface.[20−22] However, the contribution of the undulation to the increase in the interfacial area is not necessarily large; e.g., only 3% increase was observed for an interface possessing ca. 40 nm roughness in atomic force micrographs.[22]

The second assumption was confirmed by transmission electron microscopy, which showed that no micelles were formed in the present aPA/PSU systems. Theory predicts that the copolymers will stay at the interface and not escape to the bulk in the form of micelles, when copolymers symmetric in size are formed at the interface.[23]

The third assumption is based on the fact that the interface studied here is composed of a strongly immiscible polymer pair so that the interfacial thickness should be very small. Kramer assumed that the reaction proceeded in the interfacial region with the thickness of a statistical segment length (0.68 nm for PS[24]) for his highly immiscible interface (amine-rich or epoxy-rich epoxy network/PS−COOH).[13] On the contrary, Macosko assumed the thickness would be of the order of 5 nm for the immiscible interface with a small χ value (PMMA-epoxy/PS−COOH).[25]

The fourth assumption introduces the concept of formation of a two-dimensional monolayer at the interface between the polymers. The results shown in Figure 2, Figure 4a, and Figure 5a clearly indicate that there is a limiting value to the copolymer density required to saturate the interface, and this is denoted as Σ^* (chains/nm^2). In other words, the Σ^* corresponds to the number of molecules necessary to form the monolayer so that when the copolymer density reaches this value, the reaction will be terminated.

Kinetic Equations. The reaction at an interface with limited space can be described by the following equations:

$$r_{AB} = k_{AB}[A_{interface}][B_{interface}] \text{ [vacant sites available for the reaction at the interface]} \quad (5)$$

$$r_{AB} = k_{AB}(C_A - C_{AB})(C_B - C_{AB})(C_{AB}^* - C_{AB}) \quad (6)$$

$$r_{AB} = k_{AB}(C_A - C_{AB})(C_B - C_{AB})\Sigma^*(1 - \theta) \quad (7)$$

where k_{AB} is the rate constant, C_{AB} and C_{AB}^* are the concentration of copolymers formed at time t and at infinite time, C_A and C_B are the concentration of A and B reactive groups prior to the reaction, respectively, and θ is the fractional coverage ($\equiv\Sigma/\Sigma^*$). The values of C_A and C_B can be considered as the numbers of reactants per unit area located within the distances of $2\sqrt{D_A t_c}$ and $2\sqrt{D_B t_c}$, respectively, from the interface, where D_A and D_B are the self-diffusion coefficient of the reactive chains carrying A and B, respectively, and t_c is the reaction time needed to reach the Σ^*. For the special case where one phase does not have diffusivity (e.g., the phase containing the reactant B), C_B is considered to be $[B_{interface}]^0$. Namely, the number of reactants in the vicinity of the interface, which can participate in the coupling reaction, is taken into consideration.

Therefore, it is more precise to rewrite eq 4 for the coupling reaction at the immiscible polymer−polymer interface as follows, which indicates that two processes take place at the same time:

$$A_{interface} + B_{interface} \rightarrow A{-}B_{interface} \quad \theta \text{ varies from 0 to 1} \quad (8)$$

Reaction Models Possessing Pseudo-First-Order Kinetics. To clarify the reaction mechanism applicable to the experimental results given in the previous section, two kinds of pseudo-first-order kinetic equations are proposed, from which three reaction models are deduced.

Kinetic Equation I:

$$r_{AB} = k_{AB}C_AC_B\Sigma^*(1-\theta) \quad (C_A \gg C_{AB},\ C_B \gg C_{AB}) \quad (9)$$

Equation 7 is of pseudo-first-order kinetic form, when $C_A \gg C_{AB}$ and $C_B \gg C_{AB}$, in which case the reaction rate decreases linearly with the fractional coverage, θ, during the reaction. The equation also indicates that the time dependence of $\Sigma \sim -\exp(-t)$. This situation applies when the spatial restriction at the interface terminates the reaction, despite reactive groups A and B being abundant in the system. Thus, the interface at the end of the reaction is densely covered by the copolymers generated by the reaction. The copolymers are formed using both $A_{interface}$ and $B_{interface}$, as illustrated by model I in Figure 7. A in △ (or ▲ in the lower figure) and B in ○ (or ● in the lower figure) in the upper figure indicate reactive groups located on the interface plane, i.e., corresponding to $A_{interface}$ and $B_{interface}$ in eqs 2 and 3, respectively. The open and closed marks used in the lower figure denote unreacted and reacted groups located on the interface plane, respectively. The arrows with a solid line and a dotted line indicate the movement from above the interface plane and the movement from below the interface plane, respectively.

Model I is widely applicable to ordinary interfaces, if the two component polymers with abundant reactants have substantial diffusivity at the annealing temperature. At the end of the reaction, the copolymers are in the form of a densely packed brush and would have a stretched conformation, as predicted by Leibler.[26]

Kinetic Equation II. Kinetic equation II is a special case of kinetic equation I. Although eq 9 is applicable to the case where the spatial saturation of the interface by copolymers formed in situ terminates the reaction, the next equation is applicable to the case where unavailability of one of the reactants (e.g., B) terminates the reaction. Therefore,

$$r_{AB} = k_{AB}[A_{interface}]$$
[B available for the reaction at the interface] (10)

Since the availability of the reactant B determines the termination of the reaction,

$$r_{AB} = k_{AB}[A_{interface}]\Sigma^*(1-\theta) \quad (11)$$

$$r_{AB} = k_{AB}(C_A - C_{AB})\Sigma^*(1-\theta) \quad (12)$$

Then, in order for eq 12 to become a pseudo-first-order equation,

$$r_{AB} = k_{AB}C_A\Sigma^*(1-\theta) \quad (C_A \gg C_{AB}) \quad (13)$$

Two situations, which follow eq 13, are described next. The first situation, model II, involves the case where the reactant B in the bulk cannot be provided to the interface because of lack of diffusivity of the reactive chains carrying the reactant B. The second situation, model III, is a case where the concentration of B is so low that the shortage of the reactant B terminates the reaction.

In model II, the reaction would proceed such that the reactive group A filled randomly the limited number of unreacted sites B located on the interface plane, as illustrated in Figure 8. By contrast, the $A_{interface}$ shown as △ in the figure cannot participate in the reaction because the reactive group B in the bulk does not diffuse

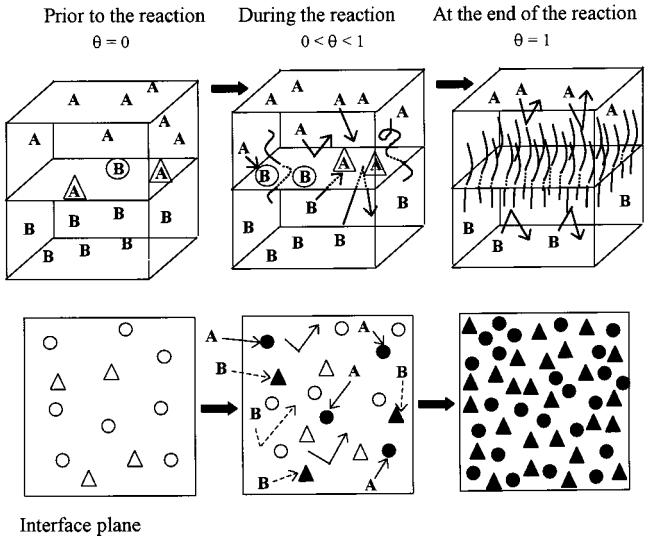

Figure 7. Scheme of model I: A in △ (or ▲) and B in ○ (or ●) are reactive groups located on the interface plane. The open and closed marks denote unreacted and reacted groups located on the interface plane, respectively. The wavy lines are copolymers formed at the interface [conditions: A, B = movable; C_A, $C_B \gg C_{AB}$].

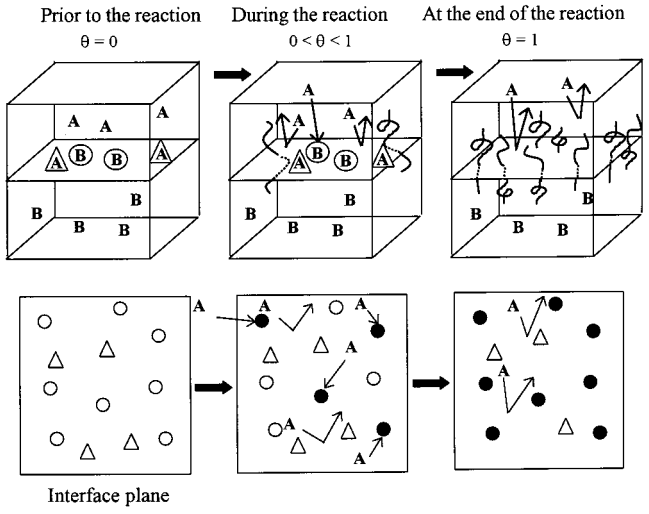

Figure 8. Scheme of model II. The symbols are the same as those used in Figure 7 [conditions: A = movable, B = unmovable; $C_A \gg C_{AB}$].

to the interface. Therefore, the initial amount of B groups on the interface, $[B_{interface}]^0$, determines the final amount of copolymers generated, and if all reactive sites of B at the interface are available for the reaction without any steric hindrance, $\Sigma^* = [B_{interface}]^0$. In a case of low $[B_{interface}]^0$, the interface is only sparsely covered by copolymers so that the copolymers are allowed to take a relaxed conformation. This model is only applicable to the interface composed of two component polymers whose glass transition temperatures differ by a large amount, and one of the phases hardly has diffusivity at the reaction temperature.

In the next model, model III, a shortage of the reactant B will stop the reaction, even though the diffusivity of both reactants is substantial. In other words, C_B determines the end point of the reaction, and if all B reactants are consumed for the reaction without any hindrance, $\Sigma^* = C_B$. As illustrated in Figure 9, the copolymers are formed using both $A_{interface}$ and $B_{interface}$, which is a different situation from model II. The

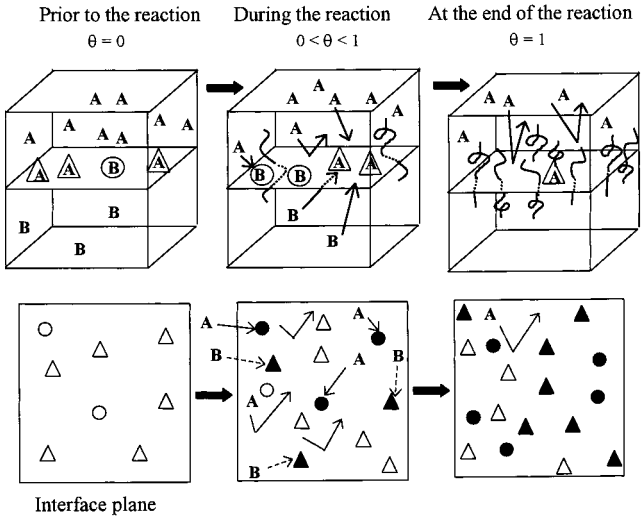

Figure 9. Scheme of model III. The symbols are the same as those used in Figure 7 [conditions: A, B = movable; $C_A \gg C_B$, C_{AB}].

Table 2. Predicted Order of Reaction Kinetics in Eq 7 under the Reaction-Controlled Mechanism[a]

reaction-controlled	kinetics
$C_A \approx C_B \approx C_{AB}$	3rd order
one of C_A and $C_B \approx C_{AB}$ and the other $\gg C_{AB}$	2nd order
C_A, $C_B \gg C_{AB}$	1st order

[a] The reaction is terminated by interfacial saturation.

Table 3. Predicted Order of Reaction Kinetics in Eq 12 under the Reaction-Controlled Mechanism[a]

reaction-controlled	kinetics
$C_A \approx C_B \approx C_{AB}$	2nd order
$C_A \gg C_{AB}$ and $C_B \approx C_{AB}$	1st order
C_A, $C_B \gg C_{AB}$	eq 7 would be applied

[a] The reaction is terminated by unavailability of the reactant B.

copolymers take a relaxed conformation at a low C_B value, similar to model II.

Rate-Determining Step and Order of Reaction Kinetics. In this section some general aspects of the coupling reaction will be discussed, including the rate-determining step of the overall coupling reaction and the concentration and diffusion of the reactants.

Despite whether the kinetics are reaction-controlled or diffusion-controlled, the reaction rate can be predicted by the behavior of each concentration term in eqs 7 and 12 during the coupling reaction. Table 2 and Table 3 summarize the predicted order of reaction kinetics under the reaction-controlled mechanism. In the former equation with three concentration terms applicable to a reaction terminated by the interfacial saturation, the order of the reaction kinetics could vary from first order to third order depending on the concentration of the reactants and products. On the other hand, in the latter equation with two concentration terms applicable to a reaction terminated by the unavailability of one of the reactants, the kinetics could be either first order or second order.

In the diffusion-controlled mechanism the reaction would first occur using the reactants located in the vicinity of the interface. Then, reactant depletion at the interface would require diffusion of the reactants to the interface in order to have further reaction. At this stage it might take some time to establish a concentration gradient between the interface region and the bulk. Then, the reaction would be impeded by interfacial saturation or by difficulty in finding the counterpair. At the end of the reaction, the reaction would be terminated either by interfacial saturation or by the depletion of one reactant, as described previously. These processes would be similar to the three time regimes proposed by Fredrickson and Milner,[6] in which simple first-order kinetics could not describe the overall kinetics. In the diffusion-controlled mechanism not only the last term in eqs 7 and 12 but also at least one concentration term of the reactants would become variables, changing with time and resulting in either second-order or third-order kinetics. Therefore, the finding of the first-order kinetics observed in the Results section implies that the overall coupling kinetics are reaction-controlled, with the reaction rate to fill the sites available at the interface being the rate-determining step. Actually, all systems cited in the previous section contained high reactant concentrations, most likely fulfilling the conditions of C_A, $C_B \gg C_{AB}$.

Furthermore, the activation energy is another piece of important information to judge whether the coupling kinetics are controlled by reaction or diffusion. For example, the diffusion-controlled mechanism usually has a low activation energy of <30 kJ/mol because it involves a physical process, whereas the reaction-controlled mechanism has a higher activation energy because it involves a chemical process. Therefore, the calculated activation energy of 120 kJ/mol for the reaction at the SMA/ATBA interface in Figure 4 strongly suggests that the coupling kinetics are reaction-controlled. The value of the activation energy agrees with the literature value for imide formation in solution.[27,28] Importantly, some other papers also reported that the coupling reaction at the immiscible polymer−polymer interface was reaction-controlled, not diffusion-controlled, from their experimental results.[13,14]

Last, there are a few things to comment in Tables 2 and 3. C_A and C_B used so far in the equations were considered as the numbers of the reactants in the region where all reactants had a potential to participate in the reaction. For example, at high reactant density of both A and B attached to short chains, the reactants are constantly supplied to the interface so that diffusion of the reactants shown by eqs 2 and 3 would not be limiting, giving rise to a reaction-controlled mechanism. On the contrary, at low reactant density with the functional groups attached to long entangled chains it would take a long time for the reactant to reach the interface to participate in the reaction so that the reaction would be more likely controlled by a diffusion process. Thus, the reaction conditions could affect the reaction mechanism as well.

Conclusions

The coupling reaction at the immiscible polymer−polymer interface has usually been treated as a second-order reaction in the literature. However, in our survey of published work and our own experiments it was demonstrated that first-order kinetics in $(\Sigma^* - \Sigma)$ were widely observed regardless of the kind of reactive pairs and the architecture of the resultant copolymers. With this information, new reaction models and kinetic equations were proposed on the basis of the concept of a two-dimensional monolayer formation. It was suggested that the coupling process with pseudo-first-order

kinetics was probably reaction-controlled, where the process to fill vacant sites available for the reaction at the interface was considered to be the rate-determining step. This means that spatial restriction at the interface plays an important role and implies a significant difference from the analogous reactions in solution. It is notable that a reaction mechanism observed for small molecules at a surface (e.g., gas/solid) can be applied to the coupling reaction in a macromolecular system.

Acknowledgment. The authors thank Prof. Kenzi Tamaru, emeritus professor at University of Tokyo, for fruitful discussion on reaction kinetics and Dr. Martin Weber at BASF Polymer Research Laboratory in Ludwigshafen, Germany, for a gift of PSU samples.

References and Notes

(1) Utracki, L. A. *Polym. Eng. Sci.* **1982**, *22*, 1166.
(2) Coran, A. Y.; Patel, R. *Rubb. Chem. Technol.* **1983**, *56*, 1045.
(3) Paul, D. R., Bucknall, C. B., Eds. In *Polymer Blends*; Wiley: New York, 1999; Vol. 1, p 539.
(4) Ide, F.; Hasegawa, A. *J. Appl. Polym. Sci.* **1974**, *18*, 963.
(5) Fredrickson, G. H. *Phys. Rev. Lett.* **1996**, *76*, 3440.
(6) Fredrickson, G. H.; Milner, S. T. *Macromolecules* **1996**, *29*, 7386.
(7) O'Shaughnessy, B.; Sawhney, U. *Phys. Rev. Lett.* **1996**, *76*, 3444.
(8) O'Shaughnessy, B.; Sawhney, U. *Macromolecules* **1996**, *29*, 7230.
(9) O'Shaughnessy, B.; Vavylonis, D. *Europhys. Lett.* **1999**, *45*, 638.
(10) O'Shaughnessy, B.; Vavylonis, D. *Macromolecules* **1999**, *32*, 1785.
(11) Scott, C.; Macosko, C. *J. Polym. Sci., Polym. Phys. Ed.* **1994**, *32*, 205.
(12) Norton, L. J.; Smigolova, V.; Pralle, M. U.; Hubenko, A.; Dai, K. H.; Kramer, E. J.; Hahn, S.; Berglund, C.; DeKoven, B. *Macromolecules* **1995**, *28*, 1999.
(13) Kramer, E. J. *Isr. J. Chem.* **1995**, *35*, 49.
(14) Schulze, J. S.; Cernohous, J. J.; Hirao, A.; Lodge, T. P.; Macosko, C. W. *Macromolecules* **2000**, *33*, 1191.
(15) Koch, H.; Ritter, H. *Makromol. Chem. Phys.* **1994**, *195*, 1709.
(16) Charoensirisomboon, P.; Inoue, T.; Weber, M. *Polymer* **2000**, *41*, 6907.
(17) Koriyama, H.; Oyama, H. T.; Ougizawa, T.; Inoue, T.; Weber, M.; Koch, E. *Polymer* **1999**, *40*, 6381.
(18) Boucher, E.; Folkers, J. P.; Creton, C.; Hervet, H.; Leger, L. *Macromolecules* **1997**, *30*, 2102.
(19) Shull, K. R. *J. Chem. Phys.* **1991**, *94*, 5723.
(20) Jiao, J.; Kramer, E. J.; de Vos, S.; Möller, M.; Koning, C. *Polymer* **1999**, *40*, 3585.
(21) Lyu, S.-P.; Cernohous, J. J.; Bates, F. S.; Macosko, C. W. *Macromolecules* **1999**, *32*, 106.
(22) Kuroda, T.; Torikai, K.; Oyama, H. T.; Ougizawa, T.; Inoue, T.; Weber, M. *Kobunshi Ronbunshu* **1999**, *56*, 860.
(23) Leibler, L. *Physica A* **1991**, *172*, 258.
(24) Anastasiadis, S. H.; Russell, T. P.; Satija, S. K.; Majkrzak, C. F. *J. Chem. Phys.* **1990**, *92*, 5677.
(25) Guégan, P.; Macosko, C. W.; Ishizone, T.; Hirao, A.; Nakahara, S. *Macromolecules* **1994**, *27*, 4993.
(26) Leibler, L. *Makromol. Chem. Macromol. Symp.* **1988**, *16*, 1.
(27) Padwa, A. R.; Sasaki, Y.; Wolske, K. A.; Macosko, C. W. *J. Polym. Sci., Polym. Chem. Ed.* **1995**, *33*, 2165.
(28) Levin, I. N. In *Physical Chemistry*; McGraw-Hill: New York, 1983.

MA001672C